

# Cosmic ray latitudes survey 1996–1997: 1. Cutoff rigidities for different azimuth and zenith angles

O. A. Danilova<sup>1</sup>, L. I. Dorman<sup>2,3</sup>, N. Iucci<sup>4</sup>, M. Parisi<sup>4</sup>, N. G. Ptitsyna<sup>1</sup>, M. I. Tyasto<sup>1</sup>, and G. Villoresi<sup>4</sup>

<sup>1</sup>SPbFIZMIRAN, Russian Academy of Science, St. Petersburg, Russia

<sup>2</sup>Israel Cosmic Ray Center and Emilio Segre' Observatory, affiliated to Tel Aviv University, Technion and Israel Space Agency, Israel

<sup>3</sup>IZMIRAN, Russian Academy of Science, Troisk, Russia

<sup>4</sup>Dipartimento di Fisica "E. Amaldi", Università "Roma Tre", Rome, Italy

**Abstract.** Non-vertical effective cutoff rigidities have been computed by tracing particle trajectories through the summarized magnetic field of the International Geomagnetic Reference Field model (IGRF95, IAGA Division 5 Working Group 8, 1996) and the Tsyganenko (1989) magnetosphere model. The computation was done for the first 39 days (from Italy to Antarctica) of the Italian Antarctic ship survey 1996–1997, for geographic points corresponding to the daily average coordinates of the expedition ship; for zenith angles 15, 30, 45 and 60 degrees, and azimuth angles from 0 to 360 degrees in steps of 45 degrees.

## 1 Introduction

During the 1996–1997 solar minimum we conducted a cosmic ray (CR) latitude survey on an Italian Antarctic Research Program ship, measuring the neutron intensity over the ocean using a 3NM-64 neutron monitor (NM) and two bare (BC)  $\text{BF}_3$  counters (Villoresi et al., 2000; Iucci et al., 2000; Dorman et al. 2000). In Dorman et al. (2000) cutoff rigidities of vertically incident CR particles have been calculated using a numerical trajectory method for the corresponding average geographic location of the ship and by taking into account the penumbra effect. In the same paper the authors computed the coupling functions for NM and BC detectors. Also the so-called "apparent" cutoff rigidities (see Clem et al., 1997) were computed in the dipole approximation by taking into account the contribution of particles reaching the detector from nonvertical incidence directions. In the present paper we extend the computation of cutoff rigidities to non-vertically incident CR particles in "real" geomagnetic field, to obtain

a better determination of the apparent cutoff rigidities and coupling function (see Dorman et al., this issue).

## 2. Computation of non-vertical cutoff rigidities

Cutoff rigidities of non-vertically incident CR particles have been calculated using a numerical trajectory method (McCracken et al., 1962) for every day for the corresponding average geographic location of the ship. Computations were done by considering the Earth's total magnetic field as the sum of fields generated by both internal and external sources. The main geomagnetic field from internal sources is represented by a Gaussian series with the International Geomagnetic Reference Field 1995 coefficients (IAGA Division V, Working Group 8, 1996) up to  $n=10$ , extrapolated to the epoch of the survey. Note that the secular variation of the main geomagnetic field is too small to affect the results of calculations during the survey time. The magnetic field from external sources is represented by the magnetospheric magnetic field model developed by Tsyganenko (1989). It takes into account the contribution from (1) ring current, (2) the magnetotail current system including the plasma sheet current and return currents, and (3) magnetopause currents as well as the large-scale system of field-aligned currents. Calculations were done for a quiet magnetosphere ( $K_p = 0$ ), corresponding to the "quiet" solar-interplanetary conditions observed during the survey period. For each point we computed the upper cutoff rigidity  $R_c$ , which is the rigidity value of the highest detected allowed/forbidden transition among the computed trajectories (e.g., Cooke et al., 1991), and the lowest cutoff value  $R_L$ , which is the rigidity value of the lowest allowed/forbidden transition. A trajectory was considered "forbidden" if its asymptotic longitude is bigger than  $1000^\circ$ . Calculations have been done for 0.001-GV steps. The effective cutoff rigidity  $R_{ep}$  is defined by the condition:

*Correspondence to:* Lev I. Dorman  
(lid@physics.technion.ac.il, lid1@ccsg.tau.ac.il)

$$\sum_{j=R_{cp}}^{R_c} W_j \Delta R_j = \sum_{i=R_L}^{R_c} W_i \Delta R_i (\text{allowed}) \quad (1)$$

where  $W_i$  is the coupling function in the  $\Delta R_i$  interval. Under the reasonable hypothesis of a flat  $W_i$  in the  $R_L - R_c$  interval (flat CR spectrum approximation (e.g., Shea et al. 1976)), we obtain

$$R_{cp} = R_c - \Delta R_{cp} \approx R_c - \sum_{i=R_L}^{R_c} \Delta R_i (\text{allowed}). \quad (2)$$

For this calculation we used  $\Delta R_i = 0.01$  GV intervals.

We calculated also the diurnal variations of vertical cutoff rigidities  $R_v$  for every day and found that they are smaller than 0.1 GV at geographic latitudes 40°N-40°S and smaller than 0.15 GV at latitudes 40°-53°S. In every point  $R_v$  value at 12 LT was nearly equal to the daily average. Assuming that this result could be extended also to inclined particles, we calculated the effective cutoff rigidities at 12 LT.

### 3. Results

The results of computation are given in Tables 1A and 1B. Figures 1 and 2 show an example of cutoff behavior during different days of latitude survey, from 0 to 38. It is remarkable in Figure 1 the geomagnetic field anomaly encountered on the forth day of survey, discussed by Dorman et al. (2000).

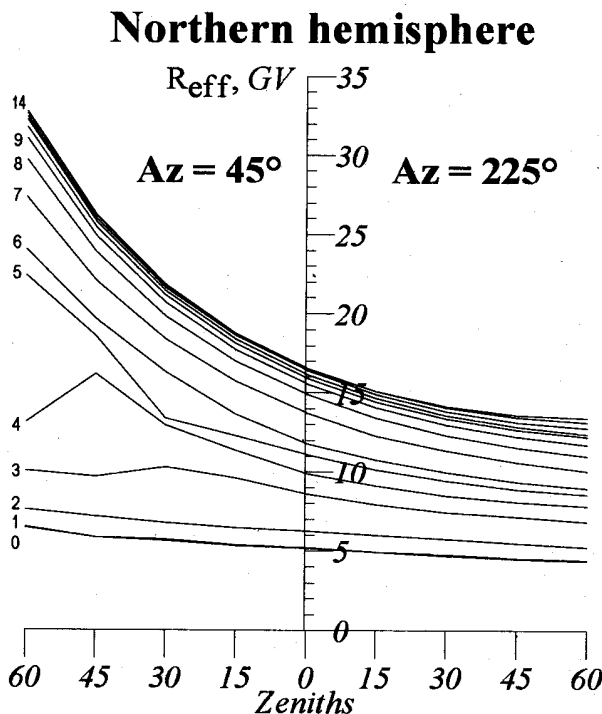


Figure 1. Effective cutoff rigidity profiles computed for the first 15 days of survey (Northern hemisphere) for different zenith angles and opposite azimuth angles.

### Southern hemisphere

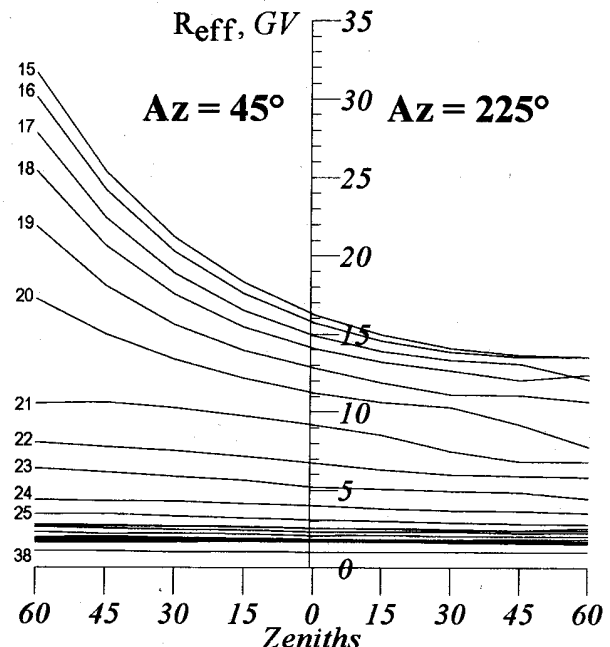


Figure 2. Same as in Figure 1, for Southern hemisphere.

### References

- Clem, J.M., Bieber, J.W., Duldig, M., Evenson, P., Hall, D., and Humble, J., J. Geophys. Res., 102, 26,919-26,926, 1997.
- Cook D. J. et al., Nuovo Cim., 14, 213, 1991.
- Dorman, L.I., Villoresi, G., Iucci, N., Parisi, M., Tyasto, M.I., Danilova, O.A., Ptitsyna, N.G., J. Geophys. Res. 105, 21,047-21,056, 2000.
- Dorman, L.I., et al., Cosmic Ray Latitude Survey 1996-1997, 2. Apparent Cutoff Rigidities, Proc. 27<sup>th</sup> ICRC, this issue.
- IAGA Division 5, Working Group 8, "International Reference Field 1995 Revision", Pure Appl. Geophys., 147, 195-202, 1996.
- Iucci, N., Villoresi, G., Dorman, L.I., Parisi, M., J. Geophys. Res. 105, 21,035-21,045, 2000.
- McCracken, K.G., Rao, U.R., and Shea, M.A., The trajectories of cosmic rays in a high degree simulation of the geomagnetic field, M.I.T. Tech. Rep. 77, Lab. for Nucl. Sci. and Eng., Mass. Inst. of Technol., Cambridge, 1962.
- Shea, M.A., Smart, D.F., and Carmichael, H., Summary of cutoff rigidities calculated with the International Geomagnetic Reference Field for various epochs, Rep. AFGL-TR-76-0115, Environ. Res. Pap. 561, Air Force Geophys. Lab., Bedford, Mass., 1976.
- Tsyganenko N.A., Planet. Space Sci., 37, 5-20, 1989.
- Villoresi, G., Dorman, L.I., Iucci, N., Ptitsyna, N.G., J. Geophys. Res. 105, 21,025-21,034, 2000.

**Table 1A.** Effective cutoff rigidities computed along the survey from Italy to Antarctica (first 39 days) for different zenith angles  $\theta$  (0, 15, 30, 45, 60 degrees) at different azimuth angles (0, 45, 90, 135 degrees) of incident particles.

N	Day	Lat	Lon	$\theta=0$	$\phi=0$				$\phi=45$				$\phi=90$				$\phi=135$			
					$\theta=15$	$\theta=30$	$\theta=45$	$\theta=60$												
0	355	44.443	12.247	5.15	5.10	5.11	5.66	5.06	5.34	5.65	5.85	6.46	5.55	5.96	6.29	6.75	5.49	5.72	6.01	6.14
1	356	44.402	12.382	5.19	5.14	5.17	5.34	5.04	5.36	5.73	5.85	6.50	5.55	5.93	6.37	6.84	5.43	5.73	6.00	6.14
2	357	41.757	16.556	6.26	6.08	6.08	6.08	6.79	6.46	6.79	7.14	7.59	6.73	7.27	7.75	8.30	6.67	7.05	7.31	7.59
3	358	37.25	21.264	8.61	8.78	8.01	7.73	7.96	9.58	10.27	9.66	10.03	9.82	11.45	13.89	17.08	9.25	10.00	10.76	11.30
4	359	33.857	26.881	9.89	10.70	11.18	9.21	9.22	11.36	12.93	16.20	13.14	11.26	13.12	17.49	22.76	10.80	12.17	13.67	15.69
5	360	31.557	31.921	11.10	11.05	12.42	12.15	9.93	12.29	13.36	18.55	22.40	12.76	15.99	19.84	25.54	12.05	13.31	15.54	18.04
6	361	30.061	32.548	11.82	12.16	11.65	14.25	10.40	13.64	16.31	19.63	24.03	13.96	16.96	20.94	27.01	12.84	14.56	16.59	19.46
7	362	25.651	35.413	13.78	14.45	15.41	16.12	17.66	15.72	18.36	22.05	27.33	15.94	19.05	23.62	30.55	14.92	16.63	19.17	22.92
8	363	20.816	38.544	14.91	15.56	16.62	18.12	19.98	16.97	19.82	23.85	29.69	17.30	20.74	25.77	33.37	16.26	18.30	21.31	25.74
9	364	16.493	41.145	15.58	16.18	17.22	18.76	20.86	17.70	20.67	24.89	31.03	18.13	21.77	27.08	35.09	17.11	19.37	22.67	27.51
10	365	12.844	44.252	15.95	16.49	17.49	19.03	21.17	18.09	21.12	25.43	31.75	18.60	22.35	27.82	36.06	17.60	20.00	23.47	28.54
11	366	12.239	49.683	16.18	16.72	17.75	19.31	21.51	18.35	21.42	25.80	32.21	18.86	22.67	28.21	36.55	17.85	20.28	23.81	28.96
12	1	9.728	54.71	16.43	16.94	17.93	19.48	21.69	18.62	21.71	26.15	32.66	19.17	23.06	28.69	37.15	18.18	20.70	24.34	29.64
13	2	6.278	59.323	16.56	16.99	17.90	19.38	21.51	18.71	21.79	26.23	32.76	19.33	23.25	28.92	37.43	18.38	20.99	24.72	30.14
14	3	2.82	63.9	16.50	16.84	17.65	19.00	20.98	18.59	21.60	25.96	32.42	19.27	23.18	28.83	37.27	18.38	21.05	24.83	30.30
15	4	-0.64	68.49	16.26	16.49	17.16	18.33	20.08	18.25	21.14	25.35	31.62	18.99	22.83	28.38	36.66	18.18	20.87	24.66	30.11
16	5	-4.629	73.476	15.74	15.81	16.29	17.19	18.54	17.56	20.23	24.18	30.09	18.36	22.07	27.43	35.41	17.68	20.34	24.08	29.42
17	6	-8.788	78.023	14.90	14.81	15.04	15.58	16.39	16.48	18.87	22.42	27.77	17.36	20.85	25.92	33.46	16.80	19.40	23.00	28.10
18	7	-12.023	82.657	14.06	13.83	13.84	14.05	14.34	15.42	17.50	20.62	25.36	16.34	19.62	24.38	31.50	15.92	18.42	21.87	26.71
19	8	-15.623	87.286	12.86	12.49	12.27	12.12	11.90	13.93	15.58	18.07	21.85	14.88	17.83	22.18	28.72	14.60	16.93	20.10	24.48
20	9	-18.933	91.709	11.24	10.85	10.57	10.22	9.88	12.12	13.36	14.99	17.24	13.06	15.66	19.48	25.34	12.82	15.00	17.70	21.20
21	10	-22.386	96.41	9.18	8.90	8.72	8.48	8.37	9.72	10.24	10.62	10.51	10.37	12.07	14.73	19.18	10.06	10.66	9.60	10.00
22	11	-25.862	101.473	6.72	6.89	6.95	6.93	6.99	7.15	7.52	7.77	8.04	7.23	7.68	8.17	8.83	6.97	7.23	7.63	8.30
23	12	-29.376	106.587	5.19	5.28	5.35	5.37	5.24	5.61	5.87	6.13	6.35	5.56	6.07	6.35	7.02	5.53	5.82	6.12	6.08
24	13	-32.825	111.807	4.00	4.01	3.98	3.93	3.94	4.11	4.27	4.29	4.37	4.22	4.34	4.51	4.65	4.05	4.19	4.33	4.55
25	14	-35.707	118.051	3.08	3.09	3.04	3.02	3.02	3.20	3.31	3.47	3.43	3.27	3.36	3.66	3.56	3.18	3.42	3.29	3.42
26	15	-37.818	125.015	2.52	2.51	2.55	2.57	2.52	2.60	2.67	2.73	2.76	2.56	2.69	2.82	2.87	2.58	2.62	2.66	2.74
27	16	-39.92	132.276	2.08	2.11	2.14	2.08	2.16	2.17	2.21	2.18	2.31	2.18	2.24	2.30	2.33	2.20	2.15	2.18	2.28
28	17	-42.036	139.765	1.76	1.80	1.80	1.78	1.83	1.83	1.83	1.88	1.90	1.83	1.90	1.96	1.88	1.86	1.89	1.87	1.91
29	18	-43.25	146.398	1.72	1.62	1.70	1.63	1.67	1.76	1.75	1.77	1.80	1.70	1.78	1.78	1.88	1.77	1.78	1.80	1.81
30	19	-42.881	147.341	1.73	1.77	1.76	1.73	1.82	1.83	1.85	1.88	1.84	1.88	1.89	1.94	1.99	1.83	1.94	1.82	1.97
31	20	-43.701	150.347	1.66	1.69	1.68	1.73	1.69	1.72	1.76	1.80	1.76	1.75	1.79	1.83	1.91	1.72	1.79	1.79	1.83
32	21	-45.069	158.389	1.67	1.67	1.62	1.73	1.64	1.70	1.70	1.71	1.75	1.75	1.79	1.74	1.86	1.74	1.74	1.77	1.80
33	22	-46.325	166.352	1.70	1.70	1.66	1.72	1.68	1.76	1.74	1.77	1.79	1.77	1.82	1.84	1.89	1.77	1.80	1.82	1.84
34	23	-44.349	172.3	2.29	2.34	2.32	2.31	2.35	2.43	2.46	2.53	2.60	2.45	2.50	2.58	2.87	2.44	2.51	2.74	2.61
35	24	-43.606	172.72	2.53	2.56	2.54	2.53	2.50	2.65	2.64	2.68	2.65	2.69	2.76	2.84	2.84	2.67	2.72	2.74	3.03
36	25	-43.672	172.823	2.53	2.54	2.58	2.54	2.47	2.61	2.67	2.67	2.65	2.66	2.77	2.81	2.80	2.63	2.74	2.80	2.89
37	26	-47.179	174.023	1.83	1.82	1.81	1.80	1.79	1.89	1.93	2.00	1.93	1.91	1.88	2.01	1.99	1.86	1.95	1.95	2.02
38	27	-52.628	175.464	0.98	0.99	0.98	0.99	1.00	1.03	1.01	1.05	1.05	1.03	1.05	1.12	1.06	1.02	1.08	1.04	1.09

**Table 1B.** Effective cutoff rigidities computed along the survey from Italy to Antarctica (first 39 days) for different zenith angles  $\theta$  (15, 30, 45, 60 degrees) at different azimuth angles (180, 225, 270, 315 degrees) of incident particles.

N	Day	Lat	Lon	$\phi=180$				$\phi=225$				$\phi=270$				$\phi=315$			
				$\theta=15$	$\theta=30$	$\theta=45$	$\theta=60$												
0	355	44.443	12.247	5.18	5.31	5.33	5.36	4.93	4.69	4.50	4.38	4.85	4.52	4.37	4.31	4.90	4.80	4.91	4.37
1	356	44.402	12.382	5.18	5.27	5.27	5.39	4.95	4.79	4.55	4.42	4.87	4.56	4.36	4.28	4.92	4.74	4.91	4.42
2	357	41.757	16.556	6.38	6.34	6.39	6.35	5.99	5.74	5.49	5.26	5.75	5.35	5.05	4.91	5.85	5.58	5.36	5.36
3	358	37.25	21.264	8.55	8.32	8.22	8.09	7.94	7.45	7.15	6.86	7.94	7.30	6.76	6.13	8.11	7.22	6.70	6.59
4	359	33.857	26.881	9.86	9.95	9.78	9.59	9.12	8.50	8.09	7.84	8.81	8.31	7.67	7.85	9.68	9.19	8.07	7.51
5	360	31.557	31.921	10.93	10.97	10.82	10.67	10.14	9.44	8.88	8.57	10.00	9.08	8.19	8.22	10.25	9.97	9.86	8.12
6	361	30.061	32.548	11.58	11.62	11.52	11.42	10.73	9.97	9.34	8.96	10.59	9.66	8.99	8.19	11.00	9.86	10.19	8.89
7	362	25.651	35.413	13.40	13.26	13.35	13.62	12.26	11.33	10.58	10.07	12.07	11.00	10.30	9.85	12.86	12.27	11.33	10.52
8	363	20.816	38.544	14.61	14.64	15.01	15.69	13.41	12.32	11.55	11.00	13.22	12.01	11.14	10.65	14.06	13.54	13.27	13.02
9	364	16.493	41.145	15.38	15.56	16.14	17.12	14.05	12.97	12.22	11.74	13.77	12.49	11.61	11.06	14.59	14.03	13.80	13.78
10	365	12.844	44.252	15.83	16.12	16.84	18.02	14.43	13.37	12.66	12.25	14.06	12.72	11.78	11.16	14.86	14.21	13.92	13.89
11	366	12.239	49.683	16.06	16.35	17.07	18.25	14.63	13.55	12.84	12.41	14.26	12.89	11.94	11.31	15.07	14.41	14.11	14.13
12	1	9.728	54.71	16.37	16.73	17.54	18.82	14.89	13.83	13.14	12.76	14.47	13.07	12.08	11.41	15.26	14.54	14.18	14.13
13	2	6.278	59.323	16.58	17.03	17.96	19.39	15.06	14.05	13.43	13.13	14.57	13.14	12.12	11.43	15.31	14.50	14.05	13.88
14	3	2.82	63.9	16.61	17.17	18.19	19.74	15.07	14.14	13.60	13.39	14.52	13.09	12.07	11.39	15.19	14.30	13.74	13.45
15	4	-0.64	68.49	16.47	17.11	18.23	19.87	14.93	14.09	13.65	13.54	14.31	12.91	11.93	11.28	14.89	13.93	13.28	12.86
16	5	-4.629	73.476	16.06	16.79	17.98	19.65	14.55	13.84	13.51	13.51	14.55	12.55	11.64	11.08	14.33	13.30	12.56	12.02
17	6	-8.788	78.023	15.33	16.12	17.31	18.88	13.89	13.32	13.10	12.07	13.89	11.96	11.17	10.65	13.48	12.42	11.63	11.04
18	7	-12.023	82.657	14.57	15.40	16.53	17.83	13.21	12.66	12.02	12.39	13.13	11.37	10.54	10.09	12.67	11.62	10.84	10.27
19	8	-15.623	87.286	13.39	13.97	15.04	10.96	11.86	11.11	11.07	10.64	11.43	10.30	9.55	9.05	11.52	10.54	9.86	9.43
20	9	-18.933	91.709	11.68	12.37	11.01	9.42	10.62	10.30	9.16	7.73	10.05	9.28	8.65	8.42	10.14	9.38	8.72	8.58
21	10	-22.386	96.41	9.08	8.21	7.88	8.25	8.50	7.48	6.80	6.81	8.37	7.73	7.02	6.28	8.44	7.88	7.59	7.36
22	11	-25.862	101.473	6.57	6.56	6.72	6.97	6.31	5.98	5.89	5.80	6.28	5.78	5.43	5.42	6.51	6.31	6.01	5.74
23	12	-29.376	106.587	5.26	5.27	5.28	5.08	5.04	4.90	4.83	4.43	4.96	4.75	4.56	4.51	5.09	4.85	4.68	4.61
24	13	-32.825	111.807	3.87	3.95	3.92	4.10	3.78	3.67	3.65	3.53	3.82	3.57	3.50	3.38	3.87	3.86	3.70	3.45
25	14	-35.707	118.051	3.11	3.06	3.02	3.08	3.01	2.91	2.82	2.77	2.97	2.92	2.74	2.74	3.05	2.90	2.83	2.91
26	15	-37.818	125.015	2.51	2.52	2.50	2.56	2.48	2.42	2.39	2.37	2.42	2.38	2.36	2.23	2.46	2.39	2.36	2.31
27	16	-39.92	132.276	2.13	2.08	2.23	2.08	2.09	2.03	2.02	2.02	2.03	2.00	1.92	1.92	2.11	2.03	2.02	1.91
28	17	-42.036	139.765	1.83	1.75	1.86	1.83	1.81	1.71	1.71	1.69	1.75	1.71	1.64	1.62	1.74	1.70	1.68	1.70
29	18	-43.25	146.398	1.71	1.71	1.74	1.68	1.66	1.63	1.60	1.58	1.67	1.59	1.62	1.61	1.66	1.65	1.61	1.58
30	19	-42.881	147.341	1.84	1.77	1.92	1.83	1.80	1.73	1.70	1.71	1.74	1.70	1.65	1.60	1.75	1.74	1.67	1.63
31	20	-43.701	150.347	1.68	1.70	1.71	1.72	1.69	1.63	1.60	1.56	1.67	1.60	1.57	1.61	1.70	1.63	1.56	1.60
32	21	-45.069	158.389	1.69	1.70	1.71	1.68	1.66	1.63	1.60	1.59	1.65	1.56	1.58	1.58	1.68	1.61	1.53	1.58
33	22	-46.325	166.352	1.75	1.70	1.86	1.82	1.72	1.67	1.62	1.62	1.67	1.63	1.60	1.66	1.70	1.67	1.59	1.61
34	23	-44.349	172.3	2.38	2.55	2.41	2.41	2.32	2.33	2.23	2.25	2.27	2.32	2.17	2.18	2.30	2.21	2.28	2.13
35	24	-43.606	172.72	2.61	2.55	2.69	2.60	2.53	2.46	2.36	2.54	2.46	2.31	2.37	2.29	2.51	2.43	2.39	2.40
36	25	-43.672	172.823	2.56	2.55	2.67	2.63	2.52	2.47	2.37	2.41	2.43	2.33	2.38	2.23	2.48	2.45	2.36	2.47
37	26	-47.179	174.023	1.86	1.90	1.86	1.89	1.84	1.80	1.83	1.82	1.81	1.77	1.74	1.64	1.78	1.73	1.76	1.66
38	27	-52.628	175.464	1.01	1.02	1.05	1.04	1.01	1.00	1.00	0.98	1.01	0.96	0.96	0.97	1.00	1.00	0.95	0.97